Measurement of filling factor 5/2 quasiparticle interference with observation of charge e/4 and e/2 period oscillations

R. L. Willett[1], L. N. Pfeiffer, and K. W. West

Physical Sciences Research, Bell Laboratories, Alcatel-Lucent, 600 Mountain Avenue, Murray Hill, NJ 07974

Edited by W. F. Brinkman, Princeton University, Princeton, NJ, and approved March 30, 2009 (received for review December 10, 2008)

A standing problem in low-dimensional electron systems is the nature of the 5/2 fractional quantum Hall (FQH) state: Its elementary excitations are a focus for both elucidating the state's properties and as candidates in methods to perform topological quantum computation. Interferometric devices may be used to manipulate and measure quantum Hall edge excitations. Here we use a small-area edge state interferometer designed to observe quasiparticle interference effects. Oscillations consistent in detail with the Aharonov–Bohm effect are observed for integer quantum Hall and FQH states (filling factors $\nu = 2$, 5/3, and 7/3) with periods corresponding to their respective charges and magnetic field positions. With these factors as charge calibrations, periodic transmission through the device consistent with quasiparticle charge e/4 is observed at $\nu = 5/2$ and at lowest temperatures. The principal finding of this work is that, in addition to these e/4 oscillations, periodic structures corresponding to e/2 are also observed at 5/2 ν and at lowest temperatures. Properties of the e/4 and e/2 oscillations are examined with the device sensitivity sufficient to observe temperature evolution of the 5/2 quasiparticle interference. In the model of quasiparticle interference, this presence of an effective e/2 period may empirically reflect an e/2 quasiparticle charge or may reflect multiple passes of the e/4 quasiparticle around the interferometer. These results are discussed within a picture of e/4 quasiparticle excitations potentially possessing non-Abelian statistics. These studies demonstrate the capacity to perform interferometry on 5/2 excitations and reveal properties important for understanding this state and its excitations.

5/2 fractional quantum Hall effect | fractional quantum Hall effect | non-Abelian statistics | topological quantum computation

Experimentally, the fractional quantum Hall (FQH) state at $5/2 = \nu$ filling factor is anomalous in that it occurs at an even denominator quantum number (1). The state is fragile: It displays a weak quantum Hall effect, requiring temperatures for observation substantially lower than the principal odd denominator states at $\nu =$ 1/3 and 2/3. It has been proposed as either a spin polarized [Moore–Read Pfaffian (2)] or non-spin polarized [Haldane–Rezayi (3)] paired composite fermion state. The fundamental quasiparticle excitations are expected to be charged e/4, and for the Pfaffian state these quasiparticles are to obey non-Abelian statistics. These non-Abelian states may display utility in topological quantum computational schemes (4)

To the end of determining the charge, and more importantly the statistics of the quasiparticles, interference devices and their function in displaying the Aharonov–Bohm (A–B) effect at 5/2 have been described theoretically (5–9). Interference devices are typically constructed with nominally 2 adjacent quantum point contacts (qpcs), each able to variably transmit current, and a confinement area between the qpcs (see schematic in Fig. 1). By splitting the current at the qpcs, redirection of quantum Hall edge currents around the confined area occurs. Interference of that encircling edge with the other backscattered current is expected to yield oscillatory resistance across the device for changing confinement area, with period dependent on the edge current charge. The

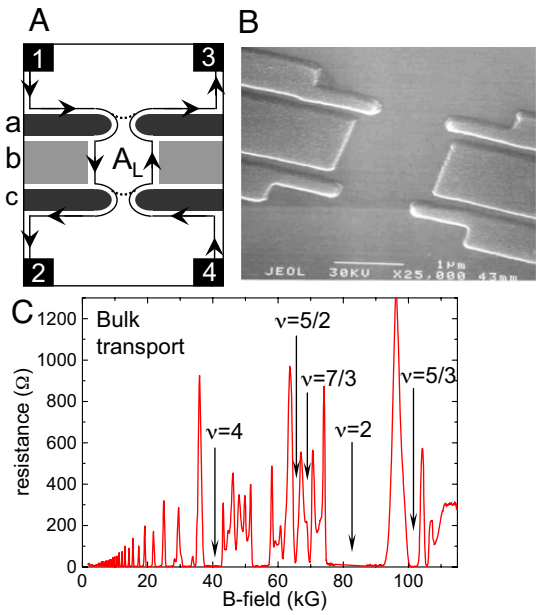

Fig. 1. Interference device and bulk sample transport. (*A*) Schematic of the interferometer showing ohmic contacts to the 2D electron layer labeled 1–4, the confined area A_L delineated by qpcs defined by gates a and c with the central channel controlled by gate b. The side-gate b voltage is referred to in these experiments as *Vs*. Longitudinal resistance (R_L) through the device could be measured by the voltage drop from 3 to 4 while driving current from 1 to 2, diagonal resistance (R_D) measured from 1 to 4 while driving current from 2 to 3. Example propagating edge states are marked by the arrows along the gates and sample edges, with the dashed lines marking where backscattering may occur at the qpcs. (*B*) Electron micrograph of an interferometer gate structure used in this study. (*C*) Bulk transport at 30 mK near but not through an interferometer device on a sample used in this study.

encircling quasiparticle statistics may also be assessed by examining the interference pattern if the confinement area holds determinable localized quasiparticles (5–9). This interferometric method is attractive in that for a given device it can be applied to a series of integer quantum Hall (IQH) and FQH states for verification of its operation through measurement of their respective charges, including the charge at 5/2 filling factor.

Edge transport interference in IQH systems has been reported for both accidental and intentional area confinements (10, 11). In

Author contributions: R.L.W. and L.N.P. designed research; R.L.W. performed research; L.N.P. and K.W.W. contributed new reagents/analytic tools; R.L.W. analyzed data; and R.L.W. wrote the paper.

The authors declare no conflict of interest.

This article is a PNAS Direct Submission.

[1]To whom correspondence should be addressed at: Bell Laboratories, Alcatel-Lucent, 600 Mountain Avenue, Room 1d-466, Murray Hill, NJ 07974. E-mail: rlw@alcatel-lucent.com.

This article contains supporting information online at www.pnas.org/cgi/content/full/0812599106/DCSupplemental.

PHYSICS

Mach–Zehnder interferometer designs (12, 13), oscillatory transmission is observed for both B-field sweep and enclosed area sweep at IQH states. FQH effect interference measurements have been more elusive. An extensive set of studies by Goldman and colleagues (ref. 14 and references therein) has reported well-defined periodic structures in interferometer transmission near FQH filling factors. Later similar studies by Godfrey et al. (15) over a filling factor range of both IQH and FQH states have shown periodic conduction, with period linearly increasing with magnetic field. These results (ref. 14 and references therein and ref. 15) are qualitatively similar, with both interference devices fabricated as etched and gated structures on the few-micrometer size scale. Such device processing supports the more robust IQH systems but may adversely affect the smaller-gapped FQH states (16). In theoretical analysis of these results and interference devices in general, Rosenow and Halperin (17) point out that periodic transmission results may be attributable to Coulomb blockade effects rather than edge state interference. This concern is of particular significance if the device fabrication adversely affects electron correlations, emphasizing the goal of developing an interferometric device that can accommodate the less robust FQH states.

Here we report interferometry studies using devices particularly designed for accommodating fragile FQH states, specifically the 5/2 state. FQH state confinement in an interferometer geometry is achieved here by using only top gate structures on ultra-high mobility, high-density samples for which the gate structures have minimal negative impact on the 2D electron quality. These top gate structures are designed to allow independent control of the size of the encircled area and the transmission qpcs, thus allowing area modulation to be used to assess quasiparticle interference. With these devices, periodic conduction oscillations are observed for both magnetic field sweeps and lateral confining gate sweeps. The oscillatory transmission observed in these studies occurs over small path lengths (approximately a few micrometers) and demonstrates phase noise. The focus of this study is the finding of periodic conduction features at $\nu = 5/2$ for lateral confining gate sweeps. At lowest temperatures, oscillation periods corresponding to charge e/4 are observed, with calibration periodic conduction at $\nu = 2$ assigned to charge e and with resistive oscillations at $\nu = 5/3$ and 7/3 having period consistent with charge e/3. The principal finding of this study is that, at 5/2 filling in addition to the e/4 oscillations at lowest temperatures, oscillations of half the e/4 period corresponding to e/2 can also be observed. Properties of these oscillations at 5/2 are shown here, including amplitude, relative prevalence, and preliminary temperature dependence. Among the possible causes, this effective e/2 period may empirically reflect the presence of an e/2 quasiparticle or may be due to a double pass of the e/4 quasiparticle around the interferometer. These results are considered within the important possible picture of non-Abelian e/4 quasiparticle statistics.

Operation of an interferometric device in the quantum Hall regime can follow in 2 modes, examining transmission while either sweeping magnetic field or sweeping device area. Phase accumulation can occur by encircling localized charge or by encircling magnetic flux quanta. In quantum Hall systems, application or retraction of the magnetic field changes both the magnetic flux density and the quasiparticle number (18), therefore influencing the phase accumulation in 2 ways, which suggests that B-field sweeps produce a somewhat complicated interferometric scheme for analysis. However, staying at fixed magnetic field but changing the encircled area size via a side gate provides a simpler method for analysis. By changing the encircled area size via a side gate, the number of encircled magnetic flux quanta is changed inducing A–B oscillations. The period of these A–B oscillations indicates the current carrying charge. Another contribution to phase accumulation will occur in this method if the change in area via the change in side gate voltage also includes a localized quasiparticle in the changed area. However, this density of localized quasiparticles is typically substantially below that of the magnetic flux density (18), with the sweep over magnetic flux lines consequently the dominant source for resistive oscillations. The side gate sweep is therefore the preferred technique given its simpler interpretation. Although a complete theoretical understanding of edge state interference is presently emerging (B I Halperin and A Stern, personal communication), it has been demonstrated experimentally (12, 13) that the area change achieved by using side-gate bias produces A–B oscillations in which the period directly reflects the charge of the edge channels. Attempts to assess the 5/2 quasiparticle charge and statistics through interferometry are therefore best served by employing a device capable of adjusting the area with a side gate while controlling the transmission independently with separately controlled qpcs.

The operation of the interferometer used here is based on generating edge current paths that are schematically shown in Fig. 1*A*: current from left contact 1 is split at qpc a, with some part of that current traversing the encircled central area A, and upon reflection at qpc c returns to qpc a via the right edge, where it interferes with the current backscattered at qpc a. By adjusting the channel voltage V_s, the central lithographic area, A_L, can be changed to encircled area A using the channel gates b. The resistance across the device (V_{3-4}) should demonstrate oscillations upon interference with period $\Delta B = \phi/A = (h/e^*)/A$ for B-field sweeps or period $\Delta A = \phi/B = (h/e^*)/B$, $\Delta A \sim V_s$ for side-gate (gate b) sweeps, again neglecting quasiparticle number change for each as described above. The device details are presented in supporting information (SI) *Text*, "Methods and Device Operation."

Bulk transport and transport through the interferometer are shown in Figs. 1*C* and 2*A*, respectively. Details of measurements are provided in *SI Text*. The bulk transport shows the lowest Landau level series of fractional states at the high B-field side of $\nu = 2$ and a well-developed 5/2 state. The longitudinal resistance through the device, R_L, is determined by using current contacts 1 and 2, and voltage drop is measured along 3–4 (19). With complete depletion under the gates at approximately −2.5 V, the qpcs and the central channel are biased negatively beyond this value for transmission, which collectively promotes observation of interference effects and adjusts total area A, respectively. The R_L data show persistence of the larger gap FQH state zero resistances through the device, and transport at 5/2 shows ≈200 Ω of backscattering or reflection at that filling factor at base temperature.

Oscillations in the longitudinal component R_L are observed in our measurements for both B-field sweeps and side-gate Vs sweeps. First, for B-field sweeps, periodic structures can be observed over a range of FQH and IQH states. Periodic structures can be coarsely observed over most of the B-field range shown in Fig. 2*A Inset*. Close examination of the resistive oscillations near $\nu = 2$ is provided by Fig. 2*A*. Here the oscillations are of period $\Delta B = 230\text{G} \pm 20$ G, which corresponds to an effective encircled area A of ≈0.2 μm^2, much smaller than the lithographically defined area. This finding is consistent with a small density gradient from depletion to full density, as might be expected with our top gate configuration. This gradual change from depletion to full density would imply that the inner edge state is well removed from the lithographic edge and therefore encloses a substantially smaller area: area $A \ll$ area A_L. Using the channel gate b, the encircled area A can be adjusted. For a change in this side-gate Vs of approximately −3 V, a 20% smaller area A can be generated (16), which resulted in an oscillation period that commensurately increased by 20%. The observation of oscillations with similar B-field period over a range of filling factors is consistent with past experimental results (ref. 14 and references therein). Given this period change with adjustment of area A, it is estimated that a side gate voltage adjustment of ≈1 mV will change the area corresponding to 1 flux quantum at B-fields near $\nu = 2$.

We turn now to the observation of resistance oscillations for variations of the side-gate voltage (Vs) for different filling factors. As noted above, a side-gate bias changes the area and so changes

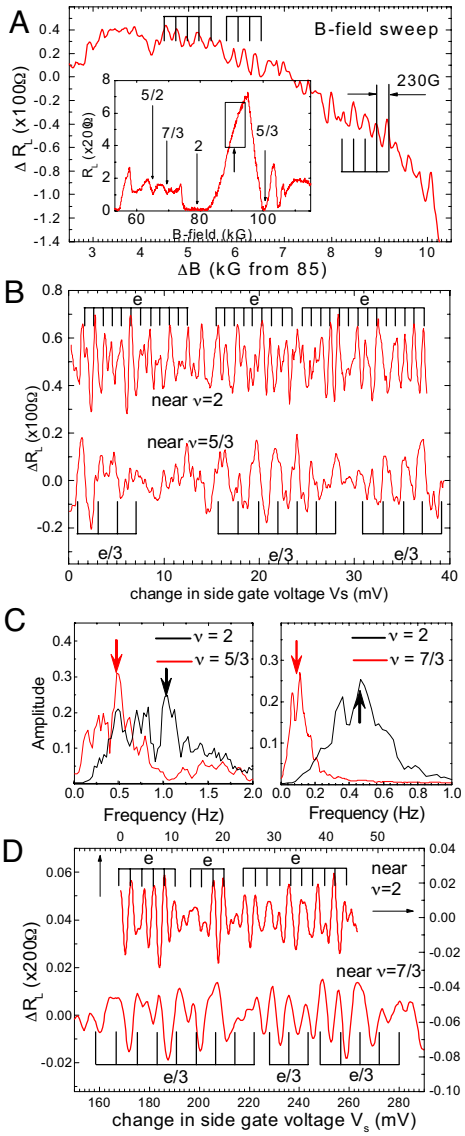

Fig. 2. Interferometer A–B oscillations: General comparison of the interferometer longitudinal resistance R_L for two types of measurement in which either the B-field is swept and resistance R_L through the device is measured, or the side-gate voltage *Vs* is swept while R_L is monitored. (*A Inset*) Overview of R_L ranging from filling factor $\nu = 3$ to near $\nu = 3/2$ with qpcs at −4.5 V bias and central channel bias at −6.0 V, temperature = 30 mK, and current = 5 nA. The box near 90 kG roughly delineates the B-field range shown in the larger graph. (*A*) Swept B-field A–B oscillations: R_L features consistent with A–B oscillations through the device with background resistance subtracted to better display the oscillations. Note runs of several oscillations, marked by the vertical lines, each with period at ≈230 G. Such runs of oscillations, with similar period, can be observed under these gating and temperature conditions throughout the magnetic field range shown in the R_L vs. B-field plot of *Inset*. (*B*) Swept side-gate A–B oscillations: R_L is monitored while sweeping the side-gate voltage *Vs* at fixed B-field. Near $\nu = 2$, runs or series of oscillations are present, with disruptions of phase between the runs. The period is marked by vertical lines reflecting the charge, period $P \sim \Delta Vs \sim \Delta A \sim (h/e^*)/B$. Each series or run of coherent oscillations is marked by the charge value. The lower trace shows a similar measurement near $\nu = 5/3$, with larger period oscillations. The vertical lines marked on that trace are the period calculated from the $\nu = 2$ period assuming $e^*(\nu = 2) = e$ and $e^*(\nu = 5/3) = e/3$, and scaling the different B-field values: $P(\nu = 5/3) = P(\nu = 2)(e^*(\nu = 2)/e^*(\nu = 5/3))(B(\nu = 2)/B(\nu = 5/3))$. The principal oscillations in the $\nu = 5/3$ trace agree well with this scaling, consistent with interferometric derivation of the fractional charge e/3 at that filling factor. (*C*) Quantitative verification of the predominant periods in swept area measurements by FFT. Left and right FFT correspond to transforms applied to the data in *B* and *D*, respectively. The principal peak frequency for each filling factor is marked by a vertical line with that frequency matched to the vertical period markers in the data of *B* and *D*. (*D*) From a different sample cool-down, a second example of A–B oscillations near $\nu = 2$ (upper trace) in which the period of those oscillations is used to determine the oscillation period for A–B oscillations at $\nu = 7/3$, matching well those features shown in the lower trace. Temperature is 25 mK, current 2 nA. Again, each run of coherent oscillations is marked by the charge, 3 coherent series for $\nu = 2$ and 3 for $\nu = 7/3$.

the number of enclosed flux quanta such that the oscillation period obeys $\Delta Vs \sim \Delta A \sim (h/e^*)/B$. To establish the relationship of period to side-gate bias, the interferometer was operated near filling factor 2, 5/3, and 7/3. Along the high field side of $\nu = 2$ near $R_L \approx 200\ \Omega$, side-gate bias is swept and R_L is measured; see typical traces in Fig. 2 *B* and *D*. All swept gate data displayed in this study correspond to measurements taken on the high B-field side of the indicated filling factor. Sequences of periodic oscillations are observed, and again come in runs or sets, rarely with >10 oscillations, but with multiple sets discernible as the side gate is swept. Such sets are marked in Fig. 2 *B* and *D* with vertical lines. The vertical lines within each set of oscillations have a single valued separation that is the measured period for that filling factor as determined by fast Fourier transform (FFT) of the side-gate sweep R_L measurement. FFT spectra of the side-gate sweep data at $\nu = 2$ are shown in Fig. 2*C*. These multiple sets of oscillations are the common observation in these measurements of R_L vs. V_S for the interferometer. The fact that long, continuous strings of oscillations are not observed may indicate that a phase disruptive noise plays a crucial role in the propagation of edge states. Despite the phase disruptions, the Fourier analysis exposes a peaked frequency spectrum, as shown in Fig. 2*C*. The peak values of the spectra are at the frequencies marked by the vertical lines in the R_L data of Fig. 2 *B* and *D*. All FFT spectra presented are extracted from the entire side-gate voltage range displayed in their respective R_L vs. V_S data figures.

The magnetic field was then adjusted so that the bulk and device filling factor are near 5/3 or 7/3, where *Vs* is then swept. The R_L vs. *Vs* spectra at these respective filling factors are displayed in the lower traces of Fig. 2 *B* and *D*. Here, the predominant period observed at 5/3 and 7/3 for several sets of oscillations in each trace is clearly larger than that of their respective traces near $\nu = 2$. This finding is verified by the Fourier spectra in Fig. 2*C* comparing filling factor 2 with 5/3 or 7/3 for the two sample preparations. By using the period from the above $\nu = 2$ traces, an oscillation period is derived for quasiparticle charge of $e^* = e/3$ given the period finding near $\nu = 2$ and considering the B-field correction for the change in flux density, $B(\nu = 2)/B(\nu = 5/3$ or $7/3)$. This expected period is marked in the 5/3 and in the 7/3 traces of Fig. 2 *B* and *D* by vertical lines of thus prescribed separation: Good agreement is observed between the large oscillatory features of the trace and the expected period for charge e/3 A–B oscillations. Again, this is supported by the Fourier spectra of the various filling factors (Fig. 2*C*), with the peak values in the FFT in agreement with the expected periods and corresponding to the marked period lines. The oscillations are observed in sets or packets that are out of phase with other packets in the same *Vs* sweep, as the runs of oscillations appear to display disruptions in phase. Given these disruptions in phase, however, the predominant oscillation features in each trace can be assigned almost completely to the A–B period of e/3. Note that in Fig. 2*D*, excluding a few minor peaks at the noise level of the measurement, all major features within the trace fall under 3 phase-shifted sets of the appropriate 7/3 period. These marked periods at 5/3 and 7/3 are placed assuming the evident phase disruptions, but the periods used are quantitatively consistent with the FFT of the data shown in Fig. 2*C*. In each case, the periods for the different filling factors derived from the FFT peak frequencies are in excellent agreement with their respective expected A–B periods.

The small effective area of the biased interferometer may particularly allow interference of fractional state excitations with small coherence lengths, as could be the case for 5/3 and 7/3. The

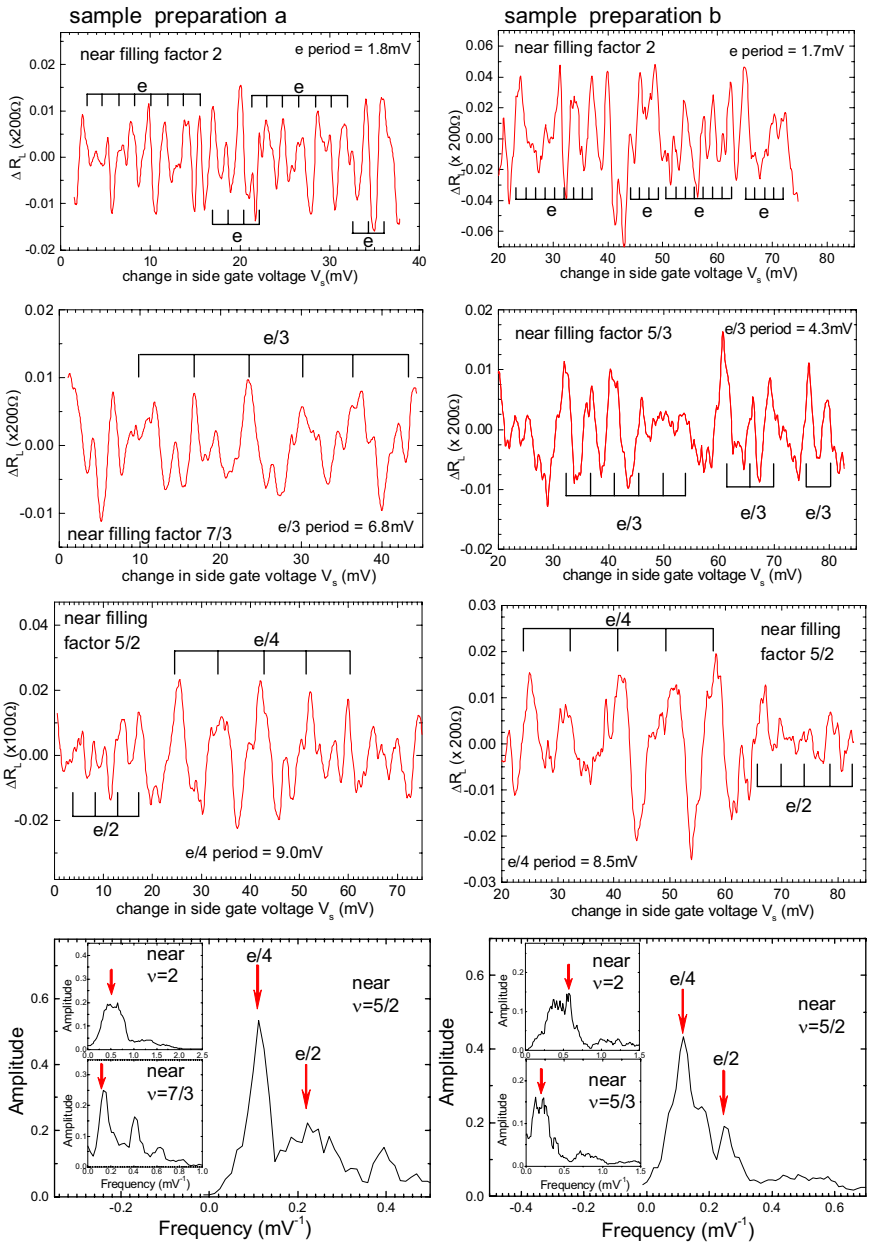

Fig. 3. A–B interferometric measurements at 5/2 filling factor displaying oscillations with periods corresponding to e/4 and e/2. R_L is measured for side-gate sweeps at filling factor $\nu = 5/2$ using similar measurements at $\nu = 2$ and 5/3 or 7/3 as metrics. Left and right columns are data at 25 mK, achieved with 2 different cool-downs from room temperature to 25 mK and using current of 2 nA. Both sides show interference effects at $\nu = 2$, 5/3 or 7/3, and 5/2, with the predominant $\nu = 2$ period marked in both by vertical lines. As in Fig. 2, this period is used to derive the period expected at 5/3 or 7/3 and additionally at 5/2 using $P \sim \Delta Vs \sim (h/e^*)/B$, assuming the quasiparticle charge of e/3 at 5/3 and 7/3, and e/4 at 5/2. Those expected periods are then marked by vertical lines in the respective traces. In both sample preparations the period of the $\nu = 2$ traces determines an e/3 quasiparticle period for the $\nu = 5/3$ or 7/3 measurement that is consistent with the predominant oscillation features in each trace. Each run or series of coherent oscillations is marked by the corresponding charge. The bottom graphs in each column show FFT of the data in the above graphs, showing frequency peaks that verify the marked period lines in the swept gate data. The bottom traces of each graph are taken near 5/2 filling and both show series of large-period oscillations. These prominent features are runs of oscillations with period consistent with quasiparticles of charge e/4 as derived from the period of the $\nu = 2$ traces; the marked vertical lines are the e/4 period derived from $\nu = 2$ and consistent with peaks of the FFT spectra. In both 5/2 traces additional oscillation features of shorter period are present that correspond to a period as expected from charge e/2, again marked by corresponding vertical lines. The amplitudes of the e/2 oscillations are generally smaller than those of the e/4, thirds, and integral filling factors. The bottom graphs show FFT spectra of the 5/2 traces, each demonstrating both e/4 and e/2 frequency peaks. Again, the arrows show the frequency/period marked in the swept gate data.

largest path length allowable in our devices, the lithographically defined perimeter, is ≈5 μm, whereas the path length corresponding to the effective area derived from B-field sweeps of 0.2 μm^2 is $2\pi r \approx 1.5$ μm.

With this validation of the interferometer operation for determining quasiparticle charge, measurements are then made near $\nu = 5/2$, with important results. Fig. 3 shows device resistance as Vs is swept at multiple filling factors, including $\nu = 5/2$ for a sample following 2 different cool-downs from room temperature to base temperature. From each cool-down, the high-mobility 2D system displays slightly different properties in standard bulk transport measurements and, likewise, displays different properties in standard transport through the interference device. For this reason we display two typical R_L vs. Vs trace sets to provide a demonstration of both the persistence of the A–B effects and the variability in the details of the traces for samples prepared differently. Additional trace sets are provided in Fig. S1, and *SI Text* includes a discussion of the high reproducibility of oscillatory features in Vs sweep data. Fig. 3 shows oscillations near $\nu = 2$, where the predominant period there is then translated to the expected period for oscillations at either $\nu = 5/3$ or $\nu = 7/3$:. These expected periods are marked in each $\nu = 5/3$ or 7/3 trace with good correspondence to oscillatory features. These are the controls for 5/2. FFT of the side-gate sweep measurements of R_L near $\nu = 2$ and $\nu = 5/3$ or $\nu = 7/3$ are shown in the insets of the bottom graphs. The peaks in the frequency spectra demonstrate quantitative agreement of the respective filling factors for expected AB oscillations.

Fig. 3 show data taken near 5/2, with evidence for e/4 charge present in both sample preparations. In each graph, at 5/2, large-period oscillations are observed at these low temperatures (≈25 mK). These prominent oscillations correspond to the e/4 quasiparticle interference. They demonstrate a good agreement in period to the period derived for e/4 quasiparticles from the $\nu = 2$ data and the data at 5/3 and 7/3. The $\nu = 2$ and 5/3 or 7/3 measured period is used to derive the anticipated period for oscillations at 5/2 for a quasiparticle charge $e^* = e/4$, with respective periods marked by vertical lines. Note that both the appropriate charge and the magnetic field scaling are necessary to achieve proper fit to the

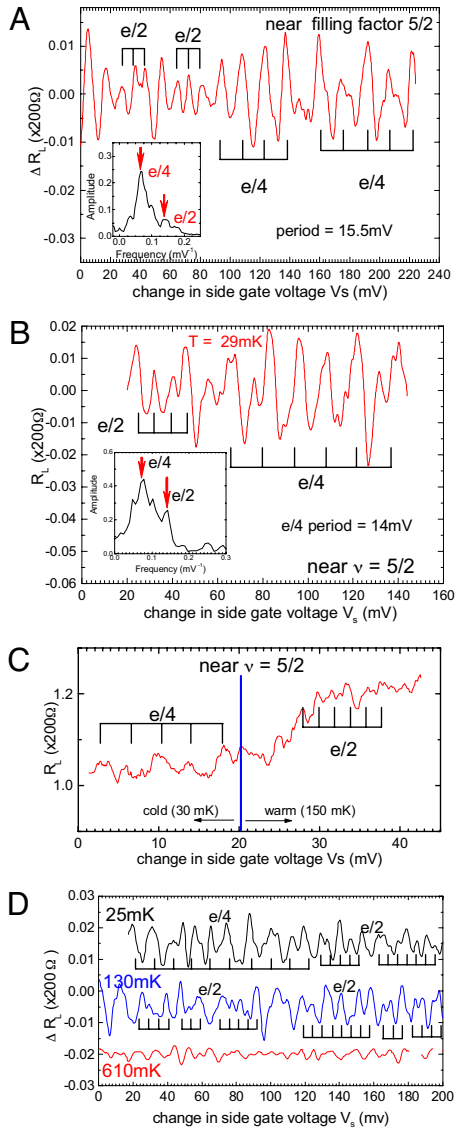

Fig. 4. Quasiparticle interference at 5/2; e/4 and e/2 period oscillations and their properties. Representative data are shown demonstrating the presence and properties of oscillations near filling factor 5/2 in R_L vs. change in side-gate voltage *Vs* measurements consistent with both e/2 and e/4 period oscillations. (*A* and *B*) Two different sample preparations demonstrating that at 29 mK within a single side-gate sweep, runs of oscillations with period corresponding to e/2 can be observed sequentially in *Vs* sweep with oscillations of period consistent with e/4, data similar to the lower traces of Fig. 3. The e/4 and e/2 periods are verified by FFT spectra (*Insets*) of the swept side-gate data, showing frequency peaks corresponding to e/4 and e/2 periods. The marked FFT peaks match the marked vertical period lines in the swept side-gate data. (*C*) Data indicate temperature dependence of e/4 and e/2 oscillations: e/2 oscillations may be made more prevalent with an increase in temperature. The temperature of the sample was taken from 30 mK to near 150 mK during a single side-gate voltage sweep with e/4 period oscillations dominant at the low temperature and e/2 oscillations present at the higher temperature. (*D*) Temperature dependence is further examined near filling factor 5/2 data from a different overall cool-down of the sample; R_L vs. *Vs* traces for the same range of *Vs* are measured at 25, 130, and 610 mK. Data are offset for clarity. The data display increased e/2 oscillations prevalence for the higher temperature (130 mK) and loss of oscillatory structure at temperatures higher than those able to support the 5/2 state, 610 mK. A current of 2 nA was used in *A*, *B*, and *D*. A current of 5 nA was used in *C*.

oscillations. Also apparent in these traces is smaller-amplitude, smaller-period oscillations, which will be addressed below. Sets of <10 oscillations with these large e/4 periods are observed, again consistent with the limited-range oscillation sets for $\nu = 2$ and $\nu = 5/3$ or 7/3. FFT data shown in the bottom graphs demonstrate peaks in the spectra at the frequency expected for e/4 given the FFT spectral peaks at filling factors 2, 5/3, and 7/3. The narrow FFT peaks corresponding to the respective thirds filling factor data provide specific determination of the expected 5/2 FFT peak position and are used in their calculation. Further examples of 5/2 data are shown in Fig. S2 *a* and *b*.

These large-period oscillations are consistent with interference of charge e/4 quasiparticles, given the correspondence in detail of charge scaling (e to e/4) and magnetic field scaling (from near $\nu = 2$ to near $\nu = 5/2$) as expected for A–B oscillations. Note that the observed oscillation periods near filling factors 5/2, 7/3, 2, and 5/3 do not respectively progress monotonically in B-field. Previous interferometer results (13) potentially attributable to Coulomb blockade possessed monotonic B-field dependence of the oscillation period, distinctly different from the results shown here. This result of e/4 charge at 5/2 is consistent with the conclusions of previous measurements of both shot noise (20) and qpc tunneling (21). These prominent oscillatory features with a period corresponding to e/4 provide substantial support for the model that the elementary excitation at 5/2 has charge e/4.

A critical finding in this study is the presence of prominent oscillations near filling factor 5/2 that display 2 different periods, the period consistent with charge e/4 and a period consistent with e/2. In the traces of Fig. 3, in addition to the oscillations of e/4 period, other distinct oscillations are apparent with a shorter period that corresponds to e/2, and are marked accordingly with appropriate vertical lines. These shorter period oscillations appear in Fig. 3 in sets or runs of oscillations adjacent sequentially in side-gate voltage to the sets of e/4 oscillations. The presence of the e/2 period is quantified by the presence in the FFT spectra of a peak corresponding to e/2, shown in the bottom graphs of Fig. 3. Further examples of such e/2 period oscillations are provided in Fig. S2 *a* and *b* including isolation of the e/2 oscillations and FFT demonstration of that period. Fig. 3 demonstrates that these e/2 period oscillations can be present at the lowest available temperatures of this study in side-gate sweeps and at side-gate voltages adjacent to those revealing e/4 oscillations. This finding is further demonstrated in Fig. 4 *A* and *B*, which show in other sample preparations additional measurements of R_L through the interferometer where the side-gate voltage *Vs* is swept. Again, in these traces 2 periods are observed, one period in size corresponding to e/4 by reference to the $\nu = 2$ period and another of half that period, which is an effective e/2 period. These data further suggest the possibility that e/4 and e/2 periods may coexist in some fashion as the side-gate is swept at the lowest temperatures available in this study.

Beyond these properties of the e/2 and e/4 oscillations, preliminary temperature dependence is displayed in Fig. 4. The top 2 graphs show typical prevalence of the e/4 and e/2 periods at the base temperature near 5/2 filling factor. The data include FFT spectra demonstrating the presence of peaks corresponding to both e/4 and e/2. The influence of temperature on the presence of this shorter period e/2 oscillation is tested in Fig. 4*C*, in which the sample temperature is changed during a side-gate sweep. The sample is first held at ≈30 mK, where large-period oscillations are observed corresponding to e/4 as marked. The sample temperature is then abruptly increased to near 150 mK, and the shorter period consistent with e/2 is exposed. These results indicate that at higher temperatures the predominant A–B period may become e/2 with diminishing occurrence of e/4 oscillations. This possibility is further examined by the data in Fig. 4*D*. Here, 3 different side-gate sweeps are performed at progressively higher temperatures. These sweeps are measured with a low drive current of 2 nA; other data collected at higher drive current is shown in Fig. S3. At lowest temperature, periods consistent with e/4 and e/2 are present. At the higher temperature of 130 mK, a greater prevalence of e/2 oscillations is observed: At this temperature the 5/2 state in bulk still demon-

strates a distinct minimum in Rxx. In these samples, the activation energy in bulk measurement is ≈150 mK. At the next higher temperature (610 mK) shown in Fig. 4*D*, the overall amplitude of the R_L measurement is substantially diminished, with only a background noise apparent. These 5/2 data suggest that, as temperature is increased, the e/2 oscillations may become the prevailing feature before elimination of the quantum Hall state above the temperature corresponding to the activation energy. The data of Fig. 4 and Fig S3 provide only a preliminary indication of the e/4 and e/2 temperature dependence.

The principal findings of this study of a small-area interferometer in which the area is changed with a side gate are as follows. (*i*) Results consistent with interference of FQH edge currents are observed and supported by data of transmission oscillations, with periods corresponding to both charge and magnetic field positions at filling factors 2, 5/3, and 7/3. (*ii*) In the model of interference of edge currents, transmission oscillations of a period appropriate to charge e/4 are demonstrated at filling factor 5/2. (*iii*) Near 5/2, an additional oscillation period corresponding to e/2 is prominent in the side-gate sweep data.

The finding of e/4 period oscillations at 5/2 is consistent with the present theoretical understanding of the 5/2 state excitations (2, 3) and their common predicted charge of e/4. This result provides a consistency with the paired state pictures of the Moore–Read state and the Haldane–Rezayi state, yet cannot discriminate between these models. Additionally, this charge assessment does not determine the underlying statistics of the excitation.

The origin of the e/2 oscillations at lowest temperatures can include empirically 2 fundamental possibilities: (*i*) the oscillations represent the presence of a quasiparticle of e/2 charge, or (*ii*) the oscillations are the result of an e/4 quasiparticle completing 2 full passes or laps around the interferometer before the interference occurs; the encircled area is doubled (the number of encircled magnetic flux are doubled) and therefore the period is halved. The first possibility, that the smaller e/2 period directly reflects the presence of e/2 quasiparticles, is not supported by early theory, which describes the elementary excitations as e/4 (2, 3, 5, 6). However, the possibility of e/2 excitations has been broached in more recent work (22). A viable picture of the presence of an e/2 quasiparticle must also include a rational for coexistence with e/4 quasiparticles and how either e/2 or e/4 period is expressed in the data sequentially, as observed in the data.

The second possibility in which e/4 quasiparticles produce both e/2 and e/4 periods, the e/2 period being caused by e/4 accomplishing 2 laps around the interferometer, has the fundamental constraint that the coherence length of the e/4 quasiparticle must be sufficient to allow completion of the longer double pass. This may be the case given the small perimeter of the interferometer and the apparent preservation of the 2D electron system high quality in the device. In addition, the generally lower amplitude of the e/2 oscillations supports this possibility. An argument against this multiple pass picture is that at higher temperatures the e/2 oscillations appear to become more prevalent, not less. Heuristically it might be expected that the larger path length of the double traversal would leave the e/2 vulnerable to thermal dephasing. The origin of the presence of the e/2 oscillations remains an open question.

Despite these difficulties, the possibility that e/4 quasiparticles doubly traverse the interferometer offers a model (5, 6) that has importance for its implications as to the statistics of the 5/2 excitations. Here the e/2 oscillations may represent a direct manifestation of the non-Abelian statistics of e/4 quasiparticles. From the theory for non-Abelian e/4 quasiparticles, if the interferometer area A encircled by the e/4 quasiparticle encloses an even number of localized quasiparticles or quasiholes, an e/4 period results: If an odd number of quasiparticles is enclosed, interference and so transmission oscillations are suppressed. Given that enclosure of an odd number of localized quasiparticles suppresses e/4 oscillations due to the non-Abelian statistics, the e/4 quasiparticles can still traverse the perimeter of the interferometer and have the potential to complete two laps around the area A. In this case, the odd number of localized particles in A has now been encircled twice, so that an even number has been encircled in sum, and interference oscillations are now not suppressed. Also, the total area encircled is now twice A, twice the encircled number of magnetic flux quanta, which would produce an effective period of e/2. Because the e/4 period from the single lap is suppressed, the e/2 period from the double lap can be expressed, but at period e/2. This picture is consistent with the sequential observation of e/2 or e/4 periods; as the side gate is swept, an odd or even number of localized quasiparticles may be enclosed. This picture also is consistent with the observation that the e/2 period oscillations are generally of smaller amplitude. Because of the longer path length that must be traversed by the quasiparticles over 2 laps, any decoherence mechanisms present will result in a concomitant amplitude reduction. The data of this study do not provide sufficient evidence to conclude this as the proper model. However, this picture is important in considering interferometric determination of potential non-Abelian e/4 excitation statistics.

In conclusion, the principal findings of this work are that interferometric measurements can be accomplished on the 5/2 FQH state: Apparent A–B oscillations are observed demonstrating periods consistent with e/4 charge for lowest temperatures tested but also demonstrating oscillation periods consistent with e/2. The origin of the e/2 oscillations is an open question. These findings of e/4 and e/2 periods may be considered in the model of non-Abelian properties of the e/4 quasiparticle.

ACKNOWLEDGMENTS. We thank B. I. Halperin, A. Stern, and H. L. Stormer for useful discussions and M. Peabody for technical assistance.

1. Willett RL, et al. (1987) Observation of an even-denominator quantum number in the fractional quantum Hall effect. *Phys Rev Lett* 59:1776–1779.
2. Moore G, Read N (1991) Nonabelions in the fractional quantum Hall effect. *Nucl Phys B* 360:362–396.
3. Haldane FDM, Rezayi EH (1988) Spin-singlet wave function for the half-integral quantum Hall effect. *Phys Rev Lett* 60:956–959.
4. Kitaev AY (2003) Fault tolerant quantum computation by anyons. *Ann Phys* 303:2–30.
5. Das Sarma S, Freedman M, Nayak C (2005) Topologically protected qubits from a possible non-Abelian fractional quantum Hall state. *Phys Rev Lett* 94:166802–166805.
6. Stern A, Halperin BI (2006) Proposed experiments to probe the non-Abelian $\nu = 5/2$ quantum Hall state. *Phys Rev Lett* 96:016802–016805.
7. Bonderson P, Kitaev A, Shtengel K (2006) Detecting non-Abelian statistics in the ν=5/2 fractional quantum Hall state. *Phys Rev Lett* 96:016803–016806.
8. Chamon C, Freed DS, Kivelson SA, Sondhi SL, Wen XG (1997) Two point-contact interferometer for quantum Hall systems. *Phys Rev B* 55:2331–2343.
9. Fradkin E, Nayak C, Tsvelik A, Wilczek F, Chern-Simons A (1998) Effective Field Theory for the Pfaffian Quantum Hall State. *Nucl Phys B* 516:704–718.
10. van Loosdrecht P, et al. (1988) Aharonov-Bohm effect in a singly connected point contact. *Phys Rev B* 38:10162–10165.
11. van Wees BJ, et al. (1989) Observation of zero-dimensional states in a one-dimensional electron interferometer. *Phys Rev Lett* 62:2523–2526.
12. Ji Y, *et al.* (2003) An electronic Mach-Zehnder interferometer. *Nature* 422:415–418.
13. Roulleau P, et al. (2008) Direct measurement of the coherence length of edge states in the integer quantum Hall regime. *Phys Rev Lett* 100:126802–126805.
14. Camino FE, Zhou W, Goldman VJ (2005) Aharonov–Bohm superperiod in a Laughlin quasiparticle interferometer. *Phys Rev Lett* 95:246802–246805.
15. Godfrey MD, et al. (2007) Aharonov–Bohm-like oscillations in quantum Hall corrals. arXiv:0708.2448v1.
16. Willett RL, Manfra MJ, Pfeiffer LN, West KW (2007) Confinement of fractional quantum Hall states in narrow conducting channels. *Appl Phys Lett* 91:052105–052107.
17. Rosenow B, Halperin BI (2007) Influence of interactions on flux and back-gate period of quantum Hall interferometers. *Phys Rev Lett* 98:106801–106804.
18. Heinonen O, ed (1998) *Composite Fermions: A Unified View of the Quantum Hall Regime* (World Sci, Singapore).
19. Beenaker CWJ, van Houten H (1991) Quantum transport in semiconductor nanostructures. *Solid State Phys* 44:1–228.
20. Dolev M, Heiblum M, Umansky V, Stern A, Mahalu D (2008) Observation of a quarter of an electron charge at the ν=5/2 quantum Hall state. *Nature* 452:829–834.
21. Radu I, et al. (2008) Quasi-particle properties from tunneling in the $\nu = 5/2$ fractional quantum Hall state. *Science* 320:899–902.
22. Wan X, Hu Z, Rezayi E, Yang K (2008) Fractional quantum Hall effect at ν=5/2: Ground states, non-Abelian quasiholes, and edge modes in a microscopic model. *Phys Rev B* 77:165316.